Density Functional Theory Studies on the Addition and Abstraction Reactions of OH Radicals with Terephthalate Dianions

NOBUAKI TANAKA, SHIGEO ITOH, HIROMASA NISHIKIORI

Department of Environmental Science and Technology, Faculty of Engineering, Shinshu University, 4-17-1 Wakasato, Nagano 380-8553, Japan

Correspondence to: N. Tanaka (E-mail: *ntanaka@shinshu-u.ac.jp*)

ABSTRACT: The addition and abstraction reactions of OH radicals with terephthalate dianions are investigated by density functional theory calculations that include solvent effects. Geometry optimizations of the reactants, products, and transition state species are performed for the potential reaction paths. For the addition reactions, those targeting the *ipso*- and *ortho*-carbons are predicted to be exoergic. The H-atom abstraction reaction is also predicted to be exoergic. On the basis of the rate constants calculated by means of the transition state theory, the H-atom abstraction reaction is determined to be the thermochemically favored path.

KEYWORDS DFT calculation; terephthalate dianion; H-atom abstraction; OH addition; transition state theory

1. INTRODUCTION

Since its proposal as a sensitive dosimeter,[1] the 2-hydroxyterephthalate dianion (HTP) has been utilized as a probe to measure OH radical generation in aqueous solutions where HTPs are generated by the reaction of terephthalate dianions with OH radicals. This method is widely used in radiochemical,[2] sonochemical,[3,4] and photocatalytic[5] reactions. Fang et al.[6] reported that OH radicals reacted with terephthalate dianions to give 2-hydroxyterephthalate dianions in 84% yield and suggested that the addition occurred at both the *ipso* and *ortho* positions in the ratio of 15:85 (*ipso:ortho*). However, no theoretical study of the detailed kinetics and thermochemistry of the reactions has been reported. In the present study, we have focused on the kinetics and thermochemistry of the primary steps; namely, OH radical addition to the terephthalate dianion and H-atom abstraction from the terephthalate dianion (Scheme 1).

2. COMPUTATIONAL METHODS

The equilibrium geometries of the reactants, transition states, products, and complexes were optimized using the density functional theory (DFT) method. Hybrid GGA functionals B3LYP[7] and mPW1PW91,[8] hybrid meta-GGA functional M06-2X,[9] and range-separated hybrid GGA functional CAM-B3LYP[10] were employed with the 6-311++G(2d,2p) basis set. As compared with the standard B3LYP functional, the mPW1PW91 and CAM-B3LYP improve long-range behavior[8,10] and the M06-2X functional has been recommended for thermochemistry and kinetics by the authors.[9] Harmonic vibrational frequencies were calculated to confirm the predicted structures as local minima or transition states (one imaginary frequency) and elucidate zero-point vibrational energy corrections (ZPE). The obtained transition states were confirmed as those connecting the investigational species by a calculation of the subsequent intrinsic reaction coordinates. The solvation effects were included using a polarizable continuum method (IEF-PCM). All calculations were performed using Gaussian 09.[11] The spin-squared values were checked, and the deviations from the doublet value of $\langle s^2 \rangle = 0.75$ were lower than 4.7%. Therefore, the spin contamination is negligible for all the studied radical species.

The rate constants for the addition and abstraction reactions were estimated using the conventional thermodynamic formulation of the transition state theory. The rate constant *k* is given by

$$k(T) = \kappa \frac{k_B T}{h} e^{-\Delta G^{\neq} / RT} \quad (1)$$

where k_B is the Boltzmann constant, *T* is the temperature, *h* is Planck's constant, $\Delta G^{\neq}$ is the Gibbs free energy of activation, and κ is the transmission coefficient. The tunneling effect was approximated using the Wigner correction.[12]

3. RESULTS AND DISCUSSION

3.1. Addition reaction

Optimized structures of the relevant stationary points for the OH addition reaction to the terephthalate dianion calculated at the UB3LYP/6-311++G(2d,2p) level of theory are shown in Figure 1. Table I lists the relative electronic energies, including the zero-point vibrational energies ($\Delta_r E$), relative enthalpies at 298 K ($\Delta_r H$), and relative Gibbs energies at 298 K ($\Delta_r G$). OH radical addition takes place at three different carbons (*ortho*, *ipso*, and carbonyl carbons) of the terephthalate dianion. For the *ortho* addition product, three stationary points (*ortho*$_1$, *ortho*$_2$, and *ortho*$_3$) were found in the CCOH torsion potential with the

following O–H directionality: *ortho*$_1$ with the O–H bond pointing toward the COO group, *ortho*$_2$ with the O–H bond pointing toward the ring, and *ortho*$_3$ with the O–H bond pointing away from the ring. For the *ipso* addition product, two stationary points (*ipso*$_1$ and *ipso*$_2$) were found in the CCOH torsion potential. For *ipso*$_1$, the O–H bond points toward the COO group and for *ipso*$_2$, it points toward the ring. Two stationary points were also found for the carbonyl addition product (carbonyl$_1$ and carbonyl$_2$). For carbonyl$_1$, the O–H bond points away from the ring and for carbonyl$_2$, it points toward the ring. The energies of the two conformers of the carbonyl addition products lie above those of the *ortho*- and *ipso*-addition products. The additions to the *ortho* and *ipso* carbons were calculated to be exoergic in contrast to the endoergic calculation for the addition to the carbonyl carbon. The spin density of the carbonyl addition product is localized on the oxygen atoms of the OH added COO group, whereas those of the *ortho*- and *ipso*-addition products are delocalized. The *ortho*- and *ipso*-addition products gain the resonance stabilization energies. The most stable conformers of the *ortho*- and *ipso*-addition products, *ortho*$_1$ and *ipso*$_1$, form an intramolecular hydrogen bond with CO···HO distances in the range of 1.708 (mPW1PW91) to 1.826 (M06-2X) Å and 1.754 (mPW1PW91) to 1.812

(M06-2X) Å, respectively.

Optimized structures of the transition states for the OH addition reactions calculated at the UB3LYP/6-311++G(2d,2p) level of theory are shown in Figure 2. Transition states TS_{ortho1}, TS_{ortho2}, TS_{ipso1}, TS_{ipso2}, $TS_{carbonyl1}$, and $TS_{carbonyl2}$ correspond to the formation of addition products *ortho*$_1$, *ortho*$_2$, *ipso*$_1$, *ipso*$_2$, carbonyl$_1$, and carbonyl$_2$, respectively. The imaginary frequencies, C···OH distances, and relative energies of the transition states are summarized in Table II. The C···OH distances in the transition states for the *ortho* and *ipso* addition reactions are elongated by over 40% as compared with those of the addition products, indicative of an early transition state. On the contrary, in the transition states for the carbonyl addition reaction, the C···OH distances are approximately 20% longer than the equilibrium distances in the addition products, indicative of a late transition state. The OH···OC distance and the loss of planarity between the carbonyl group and the ring plane in TS_{ortho1} and TS_{ipso1} indicate the presence of a hydrogen bond. Compared to the difference in the $\Delta_r G$ values for the formation of the *ortho*$_1$ and *ipso*$_1$ adducts, the difference in the $\Delta G^{\neq}$ values for the corresponding transition states (TS_{ortho1} and TS_{ipso1}) is larger. IRC calculations revealed that transition states TS_{ortho1} and TS_{ipso1} are

connected with complex$_1$ and TS$_{ortho2}$ is connected with complex$_2$. In complex$_1$, the O–H bond length is elongated by 4.0% (B3LYP) to 4.7% (M06-2X) as compared with that of the bare OH radical. The CO bond interacting with the OH radical is also elongated while the other CO bond is contracted as compared with that of the terephthalate dianion. The $\Delta_r G$ values for the formation of the complex$_1$ and complex$_2$ are calculated to a range from –2.6 (mPW1PW91) to –0.5 kcal mol^{-1} (B3LYP) and from 3.6 (mPW1PW91, M06-2X) to 5.2 kcal mol^{-1} (CAM-B3LYP), respectively, whereas the $\Delta_r H$ values are calculated to a range from –10.5 (mPW1PW91) to –8.5 kcal mol^{-1} (B3LYP) and from –3.7 (mPW1PW91) to –1.5 kcal mol^{-1} (CAM-B3LYP), respectively. At 298 K the formation of complex$_2$ is negligible.

The functional dependence of $\Delta_r G$ shows a similar trend for each stationary point. The value of $\Delta_r G$ increases in the order of mPW1PW91 < M06-2X ≈ CAM-B3LYP < B3LYP for the products and $\Delta G^{\neq}$, in the order of mPW1PW91 < B3LYP < CAM-B3LYP < M06-2X.

The calculated rate constants for OH addition to the *ortho*, *ipso*, and carbonyl carbons are listed in Table II. For TS$_{ortho1}$ and TS$_{ipso1}$, the rate constants were calculated using the values of $\Delta G^{\neq}$ estimated from complex$_1$. The

rate constants for the formation of *ortho*$_1$ and *ipso*$_1$ are smaller than those for *ortho*$_2$ and *ipso*$_2$, owing to hydrogen bond formation. The rate constants for the carbonyl addition are much lower than those for *ortho* and *ipso* addition owing to a large barrier height. OH addition to the *ortho* carbon is likely to be the dominant addition reaction channel. The experimental rate constant $k_{ortho,ipso}$ is 5.5 $\times$ 10^{-12} cm^3 mol^{-1} s^{-1}.[6] Thus, the calculated values using the B3LYP and mPW1PW91 functionals are close to the experimental value.

3.2. Abstraction reaction

Optimized structures of the relevant stationary points for H-atom abstraction from the terephthalate dianion by the OH radical calculated at the UCAM-B3LYP/6-311++G(2d,2p) level of theory are shown in Figure 3. Table III lists $\Delta_r E$, $\Delta_r H$, and $\Delta_r G$. H-atom abstraction of each of the four hydrogen atoms of the terephthalate dianion is equally possible. The transition states were optimized by starting from the three initial geometries in which the OH molecular axis was perpendicular to the molecular plane of the terephthalate dianion or the OH molecular axis was in the plane of the terephthalate dianion with either the H-atom or O-atom of the OH radical pointing to the carbonyl oxygen atom.

$TS_{abstract1}$ was calculated to be planar with the OH···OC distance in the range from 1.652 (mPW1PW91) to 1.708 (B3LYP) Å. $TS_{abstract2}$ was calculated to be nonplanar with the O–H bond pointing away from the carbonyl group. The breaking C–H bonds are elongated by about 15% and 12% as compared with the equilibrium C–H bond of the terephthalate dianion while the forming O–H bonds are elongated by about 30% and 38% as compared with the O–H bond length of H_2O for $TS_{abstract1}$ and $TS_{abstract2}$, respectively. The reactant-like geometry is characteristic of an early transition state. The $\Delta G^{\neq}$ values of $TS_{abstract1}$ are smaller than those of $TS_{abstract2}$ owing to hydrogen bonding stabilization; that is, following the H-atom abstraction reaction, the H_2O being released is attracted to the carbonyl group resulting in the formation of a hydrogen bond.

The calculated rate constants for H-atom abstraction are listed in Table III. The rate constants for the abstraction reaction via $TS_{abstract1}$ are greater than those for the abstraction reaction via $TS_{abstract2}$ by 3.4×10^3 (B3LYP) to 3.8×10^4 (mPW1PW91). Comparing the rate constants for the addition reactions versus the abstraction reaction, it can be concluded that the latter is the favored reaction channel for the reaction of OH with the terephthalate dianion. The 84%

yield of the 2-hydroxyterephthalate dianion from this reaction indicates that a fast reaction would follow the H-atom abstraction of the terephathalate dianion.

4. CONCLUSIONS

The kinetics and thermochemistry of the addition and abstraction reactions of OH radicals with terephthalate dianions have been investigated using DFT. Although the energies of formation of the *ortho* and *ipso* carbon addition products are calculated to be similar, the *ortho* carbon is the most reactive site for OH addition owing to a difference in the barrier heights. Hydrogen bonds present in the complex and TS species influence the reaction rates. The H-atom abstraction reaction is predicted to be exoergic and the barrier height is lower than those for the addition reactions.

References

1. Armstrong, W. A.; Facey, R. A.; Grant, D. W.; Humphreys, W. G. *Can. J. Chem.* **1963**, 41, 1575-1577.

2. Matthews, R. W. *Radiat. Res.* **1980**, 83, 27-41.

3. Price, G. J.; Lenz, E. J. *Ultrasonics* **1993**, 31, 451-456.

4. Villeneuve, L.; Alberti, L.; Steghens, J.-P.; Lancelin, J.-M.; Mestas, J.-L. *Ultrason. Sonochem.* **2009**, 16, 339-344.

5. Hirakawa, T.; Yawata, K.; Nosaka, Y. *Appl. Catal. A: General* **2007**, 325, 105-111.

6. Fang, X.-W.; Mark, G.; Von Sonntag, C. *Ultrason. Sonochem.* **1996**, 3, 57-63.

7. Lee, C.; Yang, W.; Parr, R. G. *Phys. Rev. B* **1988**, 37, 785-789.

8. Adamo, C.; Barone, V. *J. Chem. Phys.* **1998**, 108, 664-675.

9. Truhlar, D. G.; Zhao, Y. *Theor. Chem. Acc.* **2008**, 120, 215-241.

10. Yanai, T.; Tew, D. P.; Handy, N. C. *Chem. Phys. Lett.* **2004**, 393, 51-57.

11. Frisch, M. J.; Trucks, G. W.; Schlegel, H. B.; Scuseria, G. E.; Robb, M. A.; Cheeseman, J. R.; Scalmani, G.; Barone, V.; Mennucci, B.; Petersson, G. A.; Nakatsuji, H.; Caricato, M.; Li, X.; Hratchian, H. P.; Izmaylov, A. F.; Bloino, J.; Zheng, G.; Sonnenberg, J. L.; Hada, M.; Ehara, M.; Toyota, K.; Fukuda, R.; Hasegawa, J.; Ishida, M.; Nakajima, T.; Honda, Y.; Kitao, O.; Nakai, H.; Vreven, T.; Montgomery, J., J. A.; Peralta, J. E.; Ogliaro, F.; Bearpark, M.; Heyd, J. J.; Brothers, E.; Kudin, K. N.; Staroverov, V. N.; Kobayashi, R.; Normand, J.; Raghavachari, K.; Rendell, A.; Burant, J. C.; Iyengar, S. S.; Tomasi, J.; Cossi,

M.; Rega, N.; Millam, N. J.; Klene, M.; Knox, J. E.; Cross, J. B.; Bakken, V.; Adamo, C.; Jaramillo, J.; Gomperts, R.; Stratmann, R. E.; Yazyev, O.; Austin, A. J.; Cammi, R.; Pomelli, C.; Ochterski, J. W.; Martin, R. L.; Morokuma, K.; Zakrzewski, V. G.; Voth, G. A.; Salvador, P.; Dannenberg, J. J.; Dapprich, S.; Daniels, A. D.; Farkas, Ö.; Foresman, J. B.; Ortiz, J. V.; Cioslowski, J.; Fox, D. J. Gaussian 09, Revision B.01, Gaussian, Inc.: Wallingford, CT, 2010

12. Wigner, E. *Z. Phys. Chem. B* **1932**, 19, 203.

Figure captions

FIGURE 1. Optimized structures of the reactants, OH addition products, and complexes for the OH addition reaction calculated at the UB3LYP/6-311++G(2d,2p) level of theory.

FIGURE 2. Optimized structures of the transition states for OH addition reaction calculated at the UB3LYP/6-311++G(2d,2p) level of theory.

FIGURE 3. Optimized structures of the transition states and complex for H-atom abstraction reaction calculated at the UB3LYP/6-311++G(2d,2p) level of theory.

Table I. Thermochemical parameters in kcal mol^{-1} of the stationary points.

stationary point	functional	$\Delta_r E$	$\Delta_r H$	$\Delta_r G$
$carbonyl_1$	UB3LYP	3.4	2.3	12.5
	UM06-2X	2.5	1.3	11.6
	UCAM-B3LYP	2.4	1.2	11.5
	UmPW1PW91	–0.2	–1.3	9.1
$carbonyl_2$	UB3LYP	5.2	4.1	14.4
	UM06-2X	4.4	3.2	13.4
	UCAM-B3LYP	4.4	3.3	13.5
	UmPW1PW91	1.6	0.5	10.8
$ipso_1$	UB3LYP	–16.8	–17.9	–8.0
	UM06-2X	–20.6	–21.6	–11.8
	UCAM-B3LYP	–20.3	–21.5	–11.2
	UmPW1PW91	–22.1	–23.3	–12.9
$ipso_2$	UB3LYP	–11.3	–12.2	–2.7
	UM06-2X	–15.1	–16.0	–6.5
	UCAM-B3LYP	–14.4	–15.3	–6.3
	UmPW1PW91	–16.0	–17.0	–7.1
$ortho_1$	UB3LYP	–16.5	–17.7	–7.5
	UM06-2X	–19.7	–20.9	–10.7
	UCAM-B3LYP	–20.2	–21.4	–11.0
	UmPW1PW91	–22.0	–23.2	–13.0
$ortho_2$	UB3LYP	–12.6	–13.5	–3.8
	UM06-2X	–15.5	–16.4	–6.7
	UCAM-B3LYP	–15.7	–16.6	–6.7
	UmPW1PW91	–17.3	–18.2	–8.2
$ortho_3$	UB3LYP	–11.7	–12.4	–3.3
	UM06-2X	–14.4	–15.3	–5.7
	UCAM-B3LYP	–14.9	–15.6	–6.1
	UmPW1PW91	–16.3	–17.1	–7.6
$complex_1$	UB3LYP	–7.9	–8.5	–0.5
	UM06-2X	–9.4	–10.1	–1.7
	UCAM-B3LYP	–8.7	–9.3	–1.0
	UmPW1PW91	–9.9	–10.5	–2.6
$complex_2$	UB3LYP	–3.1	–3.1	3.8
	UM06-2X	–3.5	–3.6	3.6

	UCAM-B3LYP	–1.5	–1.5	5.2
	UmPW1PW91	–3.6	–3.7	3.6
$complex_3$	UB3LYP	–13.6	–13.5	–7.3
	UM06-2X	–15.6	–15.6	–9.2
	UCAM-B3LYP	–13.8	–13.8	–7.3
	UmPW1PW91	–15.7	–15.7	–9.2

–

Table II. Calculated imaginary frequencies, CO distance ratios, thermochemical parameters[1)] of the transition states and rate constants for addition reactions.

stationary point	functional	ν/cm^{-1}	$r_{C\cdots OH}/r_{C-OH}$	$\Delta E^{\neq}$	$\Delta H^{\neq}$	$\Delta G^{\neq}$	k/cm^3 molecule^{-1} s^{-1}
TS_{ortho1}	UB3LYP	332	1.39	4.2	3.7	5.9	5.2×10^{-13}
	UM06-2X	476	1.41	8.7	8.3	9.9	6.5×10^{-16}
	UCAM-B3LYP	365	1.42	6.0	5.5	7.6	3.3×10^{-14}
	UmPW1PW91	339	1.42	5.0	4.4	7.0	9.1×10^{-14}
TS_{ortho2}	UB3LYP	187	1.42	–2.9	–3.5	5.0	2.3×10^{-12}
	UM06-2X	357	1.43	0.8	0.1	9.2	2.0×10^{-15}
	UCAM-B3LYP	147	1.48	–1.3	–1.9	7.0	7.5×10^{-14}
	UmPW1PW91	112	1.49	–3.6	–4.2	4.6	4.1×10^{-12}
TS_{ipso1}	UB3LYP	309	1.41	6.7	6.4	7.9	1.8×10^{-14}
	UM06-2X	427	1.42	10.6	10.4	11.4	5.0×10^{-17}
	UCAM-B3LYP	337	1.43	8.5	8.2	9.7	8.5×10^{-16}
	UmPW1PW91	322	1.43	7.6	7.2	9.0	2.9×10^{-15}
TS_{ipso2}	UB3LYP	238	1.40	–1.4	–2.0	6.8	1.1×10^{-13}
	UM06-2X	352	1.43	1.4	0.7	10.3	3.5×10^{-16}
	UCAM-B3LYP	219	1.45	–0.1	–0.7	8.3	9.2×10^{-15}
	UmPW1PW91	210	1.45	–2.3	–2.9	6.0	4.0×10^{-13}
$TS_{carbonyl1}$	UB3LYP	473	1.17	12.3	11.2	21.5	2.1×10^{-24}
	UM06-2X	464	1.21	13.5	12.3	22.6	3.2×10^{-25}
	UCAM-B3LYP	451	1.20	12.9	11.7	22.0	9.0×10^{-25}

	UmPW1PW91	424	1.20	10.3	9.1	19.8	3.6×10^{-23}
$TS_{carbonyl2}$	UB3LYP	462	1.14	13.3	12.2	22.5	3.8×10^{-25}
	UM06-2X	452	1.19	14.3	13.0	23.7	4.9×10^{-26}
	UCAM-B3LYP	403	1.17	13.7	12.5	23.2	1.1×10^{-25}
	UmPW1PW91	375	1.16	11.0	9.7	20.5	1.0×10^{-23}

[1)] in kcal mol^{-1}

Table III. Calculated imaginary frequencies, ratios of HO and CH distances, thermochemical parameters[1)] of the transition states and rate constants for abstraction reactions.

stationary point	functional	ν/cm^{-1}	$r_{H\cdots OH}/\ r_{H-OH}$	$r_{C\cdots H}/\ r_{C-H}$	$\Delta E^{\neq}$	$\Delta H^{\neq}$	$\Delta G^{\neq}$	k/cm^3 molecule^{-1} s^{-1}
$TS_{abstract1}$	UB3LYP	1346	1.29	1.16	–4.6	–5.5	3.5	8.0×10^{-11}
	UM06-2X	1376	1.33	1.13	–1.9	–2.8	6.5	5.1×10^{-13}
	UCAM-B3LYP	1552	1.28	1.16	–3.5	–4.4	4.8	1.1×10^{-11}
	UmPW1PW91	1292	1.30	1.14	–6.5	–7.4	1.5	2.3×10^{-9}
$TS_{abstract2}$	UB3LYP	996	1.37	1.13	0.6	0.2	8.1	2.3×10^{-14}
	UM06-2X	1208	1.39	1.11	4.2	3.6	12.0	3.9×10^{-17}
	UCAM-B3LYP	1296	1.36	1.13	2.6	2.2	10.4	6.4×10^{-16}
	UmPW1PW91	954	1.39	1.12	–0.3	–0.8	7.5	6.0×10^{-14}

[1)] in kcal mol^{-1}

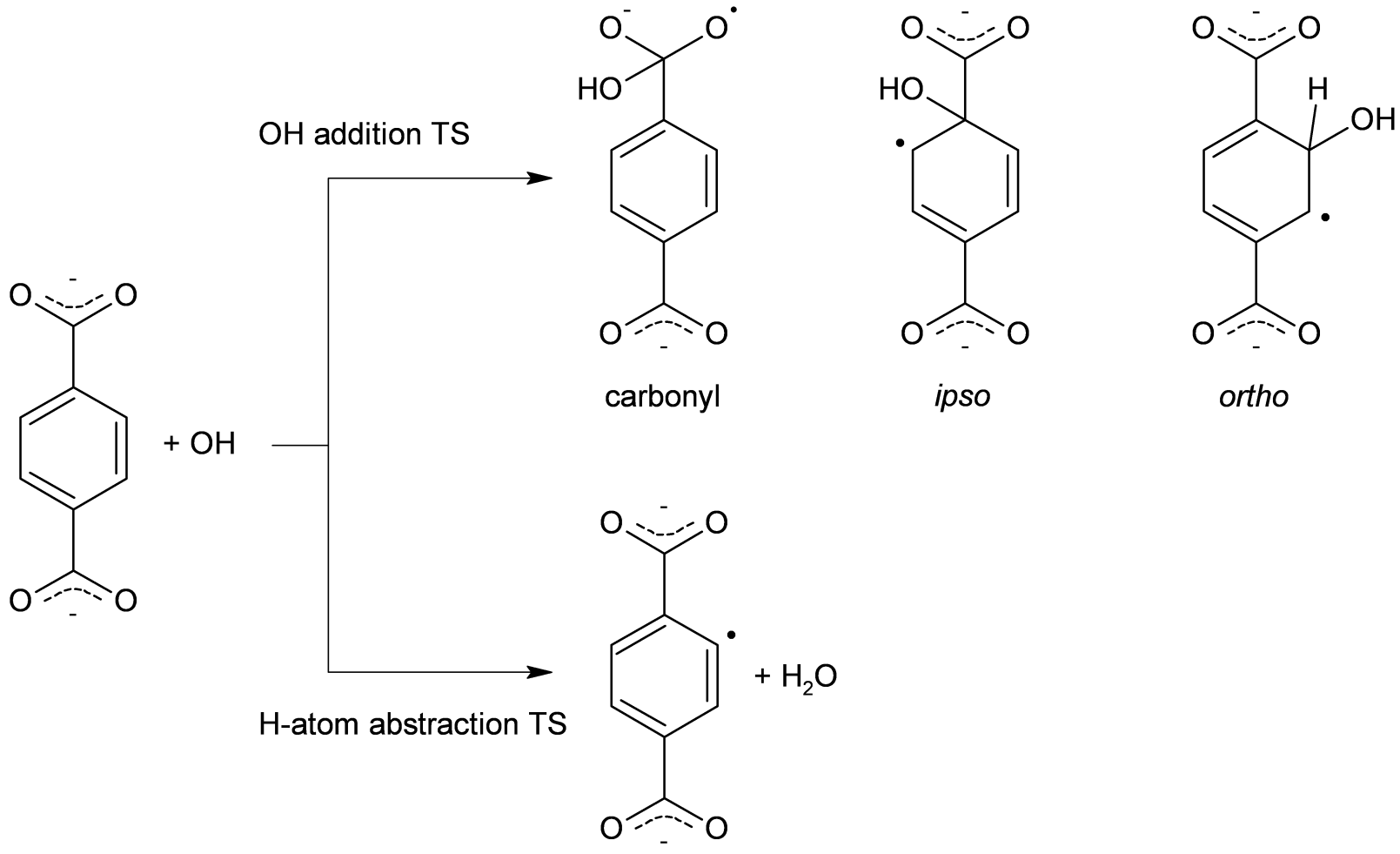
OH addition TS
+ OH
H-atom abstraction TS
+ H_2O
carbonyl
ipso
ortho

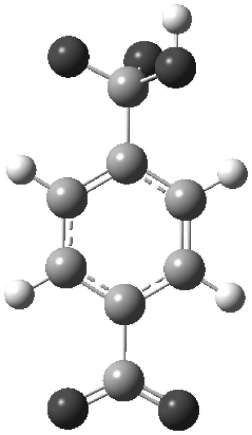

carbonyl$_1$

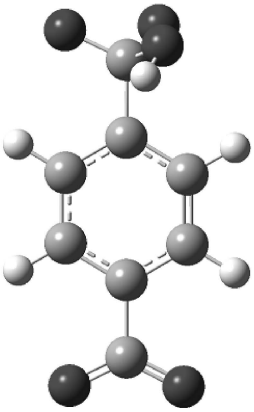

carbonyl$_2$

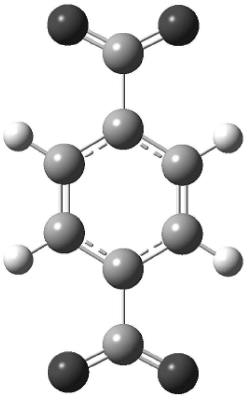

terephthalate dianion

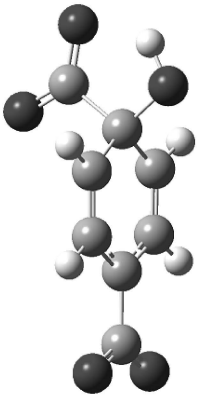

ipso$_1$

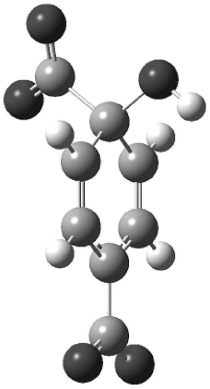

ipso$_2$

OH

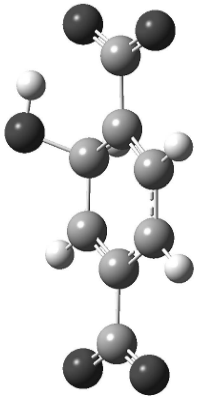

ortho$_1$

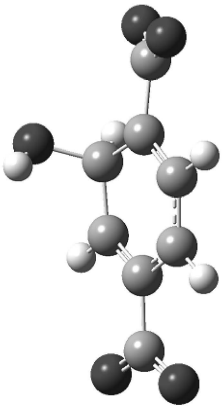

ortho$_2$

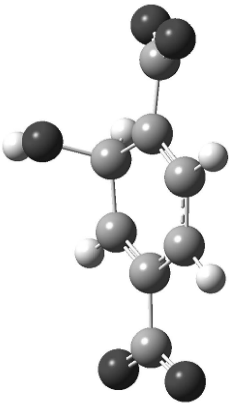

ortho$_3$

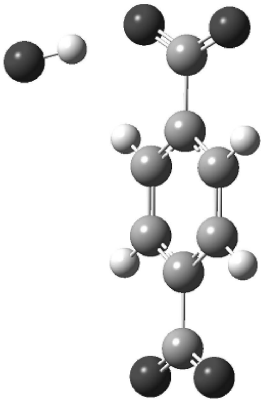

complex$_1$

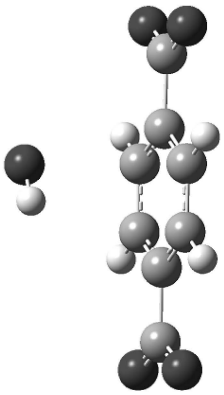

complex$_2$

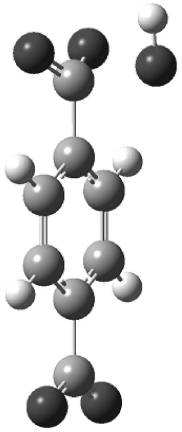

$TS_{carbonyl1}$

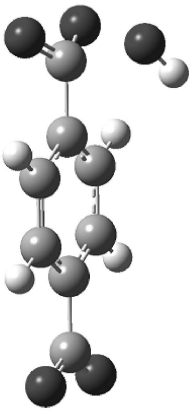

$TS_{carbonyl2}$

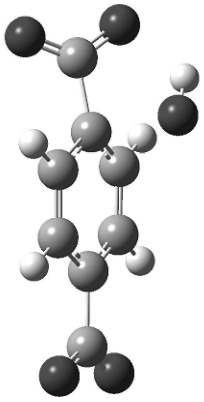

TS_{ipso1}

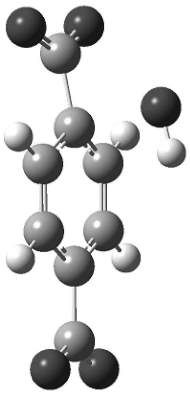

TS_{ipso2}

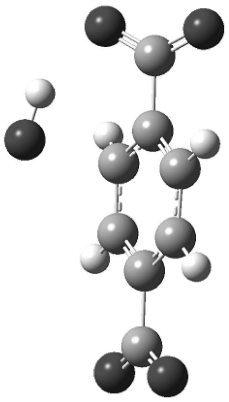

TS_{ortho1}

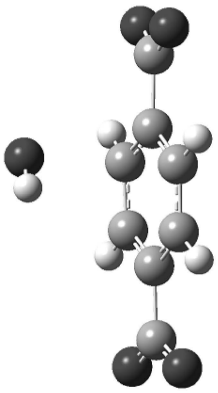

TS_{ortho2}

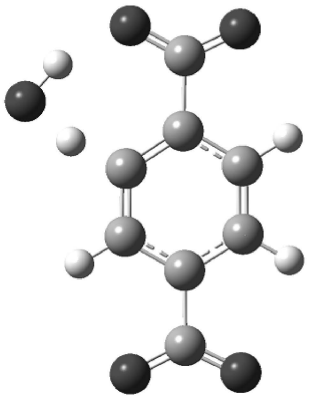

$TS_{abstract1}$

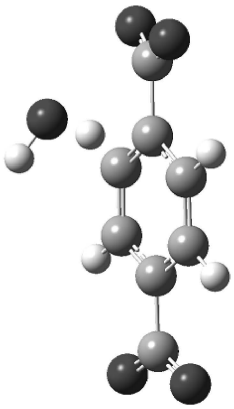

$TS_{abstract2}$

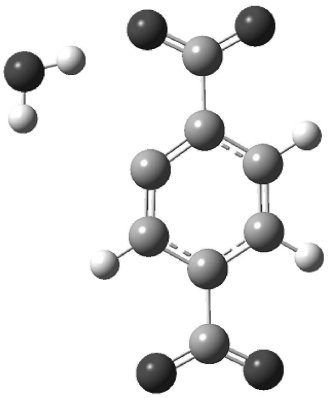

$complex_3$